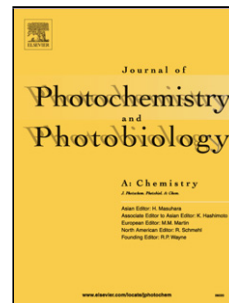


Accepted Manuscript

Title: Synthesis and photophysical investigation of 2-hydroxyquinoline-3-carbaldehyde: AIEE phenomenon, fluoride optical sensing and BSA interaction study

Authors: Nilanjan Chakraborty, Sutanwi Bhuiya, Arijit Chakraborty, Deep Mandal, Suman Das



PII: S1010-6030(18)30167-9
DOI: <https://doi.org/10.1016/j.jphotochem.2018.03.039>
Reference: JPC 11208

To appear in: *Journal of Photochemistry and Photobiology A: Chemistry*

Received date: 6-2-2018
Revised date: 26-3-2018
Accepted date: 27-3-2018

Please cite this article as: Nilanjan Chakraborty, Sutanwi Bhuiya, Arijit Chakraborty, Deep Mandal, Suman Das, Synthesis and photophysical investigation of 2-hydroxyquinoline-3-carbaldehyde: AIEE phenomenon, fluoride optical sensing and BSA interaction study, *Journal of Photochemistry and Photobiology A: Chemistry* <https://doi.org/10.1016/j.jphotochem.2018.03.039>

This is a PDF file of an unedited manuscript that has been accepted for publication. As a service to our customers we are providing this early version of the manuscript. The manuscript will undergo copyediting, typesetting, and review of the resulting proof before it is published in its final form. Please note that during the production process errors may be discovered which could affect the content, and all legal disclaimers that apply to the journal pertain.

Synthesis and photophysical investigation of 2-hydroxyquinoline-3-carbaldehyde: AIEE phenomenon, fluoride optical sensing and BSA interaction study

Nilanjan Chakraborty^{a,c}, Sutanwi Bhuiya^c, Arijit Chakraborty^{b*}, Deep Mandal^c, Suman Das^{c*}

^aDepartment of Chemistry, Maulana Azad College 8, Rafi Ahmed Kidwai Road, Kolkata 700 013, India.

^bDepartment of Chemistry, Acharya B N Seal College, Cooch Behar, West Bengal 730 161, India.

^cDepartment of Chemistry, Jadavpur University, Kolkata 700 032, India.

*To whom all correspondence should be addressed.

Suman Das

Physical Chemistry Section

Department of Chemistry

Jadavpur University

Raja S. C. Mullick Road, Jadavpur

Kolkata 700 032

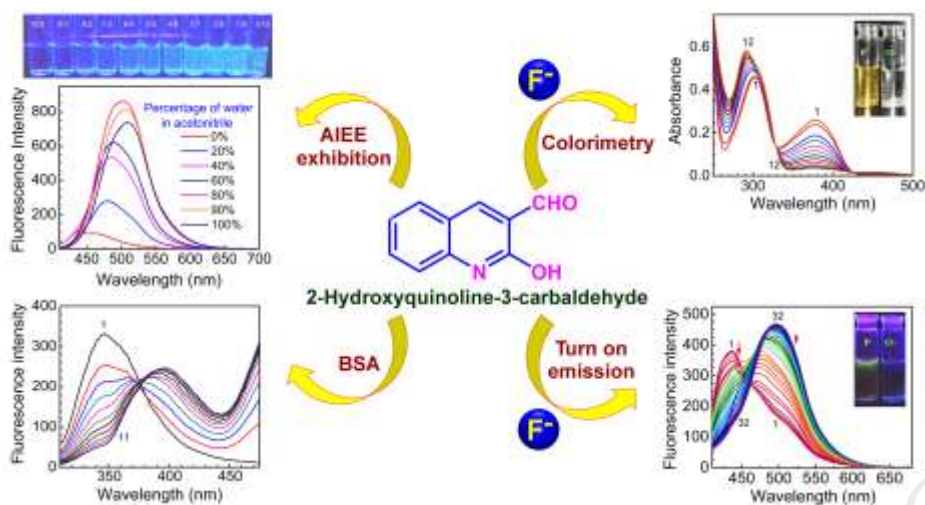
India

Tel.: +91 94 3437 3164, +91033 2457 2349

Fax: +91 33 2414 6266

E-mail:sumandas10@yahoo.com

Graphical abstract



Highlights

- Aggregation induced enhancement in emission intensity of the fluorophore 2-hydroxyquinoline-3-carbaldehyde was reported.
- Solvent effect on UV-vis and emission spectrum of the fluorophore were studied.
- The compound 2-hydroxyquinoline-3-carbaldehyde showed selective naked-eye, UV-vis and fluorescence spectral responses towards F^- ion.
- Interaction of the compound with protein bovine serum albumin (BSA) in buffer tris-HCl was reported.

Abstract

Nowadays compounds showing aggregation-induced emission enhancement (AIEE) are extensively studied due to their huge range of applications in material science. AIEE and the anion recognition ability of 2-hydroxyquinoline-3-carbaldehyde (**1**) were explored. Unique AIEE phenomenon is observed in CH_3CN with water as the cosolvent and the highest

emission was noted in the solvent volume ratio 2:8 (CH₃CN : H₂O). The compound is a selective time dependent turn on fluoride ion sensor in acetonitrile medium with a distinct color change from colorless to yellow, fabricating it as a visible sensor. Ion sensing ability was monitored through UV-vis, steady state emission, life time studies and ¹H-NMR spectroscopy. The limit of detection of fluoride ion is 4.09×10^{-6} M. Moreover the compound exhibited notable quenching of fluorescence intensity with bovine serum albumin. Thus small molecule like the quinoline motif can be used in extensive applications in the scientific research.

Keywords: 2-hydroxyquinoline-3-carbaldehyde; aggregation-induced emission enhancement; naked eye sensing; fluorescence sensor; fluoride ion, bovine serum albumin interaction.

1. Introduction

In the very recent years there have been a drift towards designing of molecular systems (fluorophores) with emission properties in solid state/ aggregate in solution. Compounds showcasing aggregation-induced emission (AIE) or aggregation-induced emission enhancement (AIEE) [1-4] have found their applications in organic light emitting devices (OLEDs) [5, 6], bioimaging applications [7, 8], nonlinear optical materials [9, 10], logic system modulation [11, 12] and many others. Generally, the fluorophores which are non-emissive or weakly emissive in nature in solution (solvents with higher solubility) emit highly upon addition of solvents like water (solvents with lower solubility) due to molecular aggregation forming hydrosol.

Among anions, fluoride ion tops the list due to its wide range of applications in biological and medicinal fields. It has been important in dental care, osteoporosis treatment *etc* [13], whereas acute exposure results in hypocalcemia, change in thyroid hormone status,

fluorosis, nervous system problems, weak bones and ligaments *etc* [14]. Fluoride being the most electronegative anion the host-guest interaction mainly occurs through hydrogen bonding [15-18], so while designing detectors this factor was kept in mind. Most of the fluoride ion detectors response colorimetrically [15-17, 19]. Many of them shows quenching [15, 17, 20] while some of them show enhancement in fluorescence intensity [16, 19, 21, 22]. In many cases they are also responsive to anions like acetate or dihydrogen phosphate [22] along with fluoride. So, designing selective and sensitive fluoride ion sensor is a challenge.

In the field of drug discovery and pharmaceutical sciences binding of various drugs to plasma protein like serum albumin is of special interest. The drug-albumin binding interaction decreases bioavailability and increases the *in vivo* half life of the drug [23]. The importance of serum albumin is due to its abundance as a multifunctional protein in blood plasma. It also act as carrier of many exogenous and endogenous compounds like fatty acids, amino acids, steroids, *etc* to blood and transport of drugs and ligands to cells [24-26]. In the family of serum albumins BSA (bovine serum albumin) being the most extensively studied one due to its repeating pattern of disulphide linkages and of about 76% of structural homology to HSA (human serum albumin) [27]. BSA is composed of 583 amino acid residues in a single polypeptide chain and is sensitive towards intrinsic fluorescence due to Tryptophan (Trp) residues Trp 134 and Trp 212 [28]. Therefore its binding affinity can be studied through fluorescence technique.

Quinoline and its derivatives have been a good fluorophore, schiff bases and other functionalities have been derived involving formyl group of 2-hydroxyquinoline-3-carbaldehyde [29] from which various metal complexes and fluorescent sensors have been developed [30, 31]. To the best of our knowledge still now 2-hydroxyquinoline-3-carbaldehyde itself have neither been targeted as fluorescent sensor nor its AIEE properties been investigated. We have synthesized

2-hydroxyquinoline-3-carbaldehyde from reported methods [32] and have proven it to be an efficient and selective turn on chemosensor for fluoride ions along with AIEE phenomenon in hydrosol form. We have also explored the studies on the interaction of this compound with BSA (bovine serum albumin) which revealed quenching of fluorescence intensity of BSA.

2. Experimental section

2.1. Materials

All solvents of analytical grade were purchased from Merck, India and reagents including tetrabutyl ammonium fluoride were obtained from Spectrochem, India and were used without further purification. Distilled water was used for AIEE studies. Bovine serum albumin (BSA) was obtained from Sigma Aldrich Corporation. By using known extinction value of $43824 \text{ M}^{-1}\text{cm}^{-1}$ at 280 nm concentration of BSA solution was determined. Tris base was obtained from Sigma Aldrich and to the 50 mM solution of the tris base appropriate amount of HCl was added drop wise to make tris-HCl buffer of pH=7.4. The buffer solution was filtered through milipore filter paper of 0.45 μm pore size. Distilled and deionized water was used throughout the experiments.

2.2. Methods

2.2.1. Physical measurements

^1H NMR and ^{13}C spectra were acquired using a Bruker 300 MHz (Bruker AVANCE 300) spectrometer and were recorded at an ambient temperature. ESI_MS was recorded on Q-tof-micro quadrupole mass spectrometer. IR spectra were obtained in KBr discs on a Spectrum Two FT-IR spectrometer in the $4000 - 400 \text{ cm}^{-1}$ region. The melting points were determined on a LabX, India Digital Melting Point apparatus and are uncorrected. All weighing was done in Mettler Toledo Analytical Balance Band (Model: MS 2045).

2.2.2. UV-vis and spectrofluorimetric studies

All UV-vis spectra of receptor were recorded in HPLC grade acetonitrile on a Perkin-Elmer UV/VIS spectrometer (Model: Lambda 25) in matched quartz cells of 1 cm path length.

Steady state fluorescence spectra were generated on a Perkin Elmer Fluorescence spectrometer (Model: LS 55). Measurements were made in fluorescence free quartz cells of path length 1 cm. All the measurements were done keeping an excitation and emission band pass of 10 nm and 5 nm. The excitation wavelength was fixed at 378 nm for anion recognition and other physical studies of compound **1**. For studies on the interaction with BSA excitation was made at 290 nm.

2.2.3. Fluorescence quantum yield measurement

The fluorescence quantum yield of the compound **1** was measured with reference to quinine sulphate in 0.1 N H₂SO₄ using the following equation [33, 34]:

$$\frac{\phi_s}{\phi_r} = \frac{I_s}{I_r} \times \frac{A_r}{A_s} \times \frac{\eta_r^2}{\eta_s^2} \text{--- (1)}$$

Where ϕ_s is the quantum yield of the sample, ϕ_r is the quantum yield of the reference used, A_r is the absorption maxima of the reference, A_s is the absorption maxima of the sample, I_r is the integrated peak area at the maximum intensity of the reference, I_s is the integrated peak area at the maximum intensity of the sample, η_r is the refractive index of the reference medium, η_s is the refractive index of the sample medium.

2.2.4. Determination of binding constant

The spectrophotometric titration data were used to construct Benesi-Hildebrand [35] plot to determine binding constant from the following equation

$$\frac{\Delta A_{\max}}{\Delta A} = 1 + \frac{1}{K[C]} \text{--- (2)}$$

$\Delta A = |A_x - A_0|$ and $\Delta A_{\max} = |A_{\infty} - A_0|$. A_0 , A_x and A_{∞} are the absorbances of compound **1** in absence of F⁻, at an intermediate anion concentration and at a concentration of complete

saturation with F^- respectively. K represents the binding constant of the complexation between compounds **1** and F^- , $[C]$ is the concentration of the variant (here in F^-). Plot was made with $\Delta A_{max}/\Delta A$ as a function of $1/[C]$. The binding constants can be obtained from the slope.

The binding constant for BSA protein binding studies was obtained from emission titration profile utilizing Benesi-Hildebrand equation:

$$\frac{\Delta I_{max}}{I} = 1 + \frac{1}{K [C]} \quad \text{--- (3)}$$

$\Delta I = |I_x - I_0|$ and $\Delta I_{max} = |I_\infty - I_0|$. I_0 , I_x and I_∞ are the emission intensities of BSA in absence of compound **1**, at an intermediate anion concentration and at a concentration of complete saturation with compound **1** respectively. K represents the binding constant of the complex formation between compounds **1** and BSA and $[C]$ is the concentration of the variant (here in compound **1**).

2.2.5. Determination of binding stoichiometry

Job's method [36] of continuous variation was employed to estimate the stoichiometry of complexation of F^- with compound **1** using absorbance spectroscopy. The difference in absorbance (ΔA) between the absorbance of free ligand and absorbance after anionic interaction was plotted against the increasing mole fraction of F^- . Sum of the concentrations of ligand and anion was maintained at 50 μM with varying their mole fractions from 0 to 1. The corresponding absorbances were taken at λ_{max} 378 nm for studies with receptor **1**. The break point in the resulting plot corresponds to the mole fraction of F^- in the $F^-:\mathbf{1}$ complex. Therefore, the stoichiometry is obtained in terms of anion:ligand [$\chi_{anion}:(1-\chi_{anion})$] where χ_{anion} is the mole fraction of anions calculated as the ratio of anions to the total molar concentration of receptors and anions

2.2.6. Limit of detection

The detection limit was calculated using calibration curve obtained from the UV-vis titration profile with the help of the equation:

$$L.O.D = \frac{3\sigma}{S} \text{---(4)}$$

Where σ is the standard deviation of the blank solution (relative absorbance ratio at 302 nm to 378 nm of 5×10^{-5} M solution of **1** in acetonitrile only), and S is the slope of the relative absorbance versus $[F^-]$ calibration curve in the lowest concentration range.

2.2.7. Fluorescence lifetime studies

Time correlated single photon counting (TCSPC) measurements were carried out in various water fractions for AIEE properties, in acetonitrile for anionic interaction and in tris-HCl buffer for BSA interaction. For both the studies the photo excitation was made at 336 nm using a picosecond diode laser (IBH Nanoled 07) in an IBH fluorocube apparatus. The fluorescence decay data were collected on a Hamamatsu MCP photomultiplier (R3809) and were analyzed by using IBH DAS6 software using the following equation [37]:

$$F(t) = \sum \alpha_i e^{-\left(\frac{t}{\tau}\right)} \text{---(5)}$$

Where, α_i is the i-th pre-exponential factor and τ is the decay time. The decay time is the life time of the excited species.

2.2.8. Synthesis

Synthesis of 2-chloroquinoline-3-carbaldehyde:

To a solution of acetanilide (5 mmoles) in dry DMF (15 mmoles) at 0-5 °C $POCl_3$ (60 mmoles) was added drop wise with stirring and the mixture was further stirred at 80-90 °C for 16 hrs. The mixture was poured into crushed ice with stirring. After 5 minutes the resulting solid was filtered, washed and dried. The compound was purified by recrystallization from ethyl acetate and the melting point was found to be 148 °C.

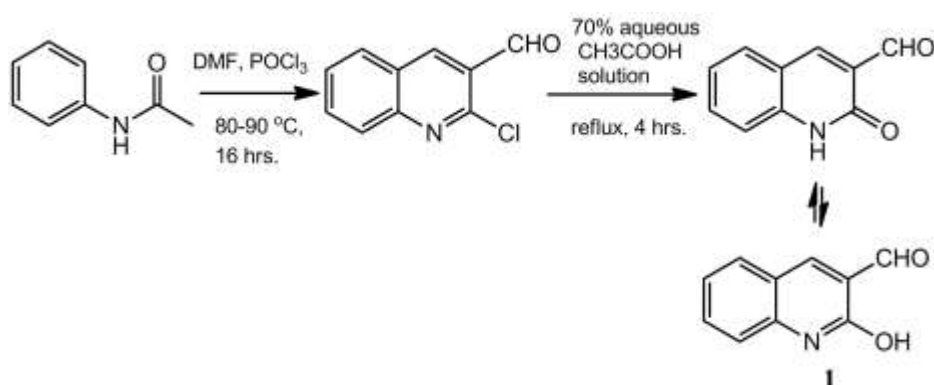
Synthesis of 2-hydroxyquinoline-3-carbaldehyde (I):

A suspension of 2-chloroquinoline-3-carbaldehyde (1 mmole) in 70% aqueous acetic acid (10 mL) was heated under reflux for 4 hours. The completion of the reaction was checked by TLC. Upon cooling the reaction mixture, a solid product precipitated out which was filtered, washed with water, dried and purified by recrystallisation from DMF. mp: 303-305°C. ^1H NMR (300MHz, DMSO- d_6): δ (ppm) 12.22 (s, 1H), 10.23 (s, 1H), 8.49 (s, 1H) 7.90 (d, $J = 7.68$, 1H), 7.64 (d, $J = 7.47$, 1H), 7.34 (d, $J = 8.25$, 1H), 7.25 (d, $J = 7.56$, 1H) (Fig. S1), FT IR (KBr) ν cm^{-1} : 3139 (N-H), 1681 (CHO), 1612 (CO) (Fig. S2), ^{13}C NMR (300 MHz, DMSO- d_6 , δ (ppm)) δ : 190.25, 161.91, 142.91, 141.63, 134.16, 131.39, 126.08, 123.13, 118.62, 115.89 (Fig. S5), HRMS (m/z): $[\text{M}+\text{H}]^+$: Calculated: 174.06, Found: 174.13 (Fig. S6).

3. Results and discussion

3.1 Synthesis

We have synthesized 2-hydroxyquinoline-3-carbaldehyde from acetanilide through the formation of 2-chloroquinoline-3-carbaldehyde by using Vilsmeier-Haack formylation method and subsequent hydrolysis of the chloro derivative (scheme 1) using methods reported in literature [32]. The compound **1** is a lactam system which can be easily converted to the corresponding iminol system. From the literature it is unclear which specific form be predominant in a particular solution condition. In fact there are several reports [30, 31, 38, 39] for the existence of both the forms. Probably, the change of tautomeric forms depends on the interaction with analyte.



Scheme 1. Synthesis of 2-hydroxy quinoline-3-carbaldehyde (**1**)

3.2. AIEE characteristics of compound 1

3.2.1. UV-vis and fluorescence studies on AIEE characteristics of compound 1

ACCEPTED MANUSCRIPT

UV-vis and emission spectra of the fluorophore **1** were taken in different proportions of CH₃CN/water (Fig. 1) to study the effect on its photo physical properties upon aggregation. Compound **1** was well dissolved in a good solvent CH₃CN where it gave a characteristic spectrum having two absorption bands at 378 and 302 nm and it displayed a moderately weak emission spectrum with emission maxima at 436 nm with a very low quantum yield of $\phi=0.0042$. With the increase in fraction of poor co solvent water emission maxima showed a positive stoke shift from 437.5 nm to 473 nm with increase in emission intensity. The positive stoke shift continued to 493 nm up to 70% of water fraction with drastic increase in emission intensity in a continuous manner. Then there was a sudden shift to 502 nm with maximum intensity (8.5 fold of intensity in pure CH₃CN) at 80% of water fraction with a $\phi=0.098$. However, upon further increase in water fraction the intensity decreases (7.2 fold of intensity in pure CH₃CN) with no further shift up to 100% of water fraction. AIEE feature was also photographed under UV lamp at 366 nm (Fig. 1C). In absorption spectra there were small

changes upon on increment of water fraction with a slight blue shift up to 370 nm from 378 nm in pure water. In our quinoline based compound **1** the free carbonyl group may serve as the rotatable unit which weaken the molecule relaxation channels for deactivation of the excitons. So in this case the enhancement of emission is probably not due to cause of restricted intramolecular rotation (RIR) but of a more generalized concept of Restricted intramolecular motion (RIM) [40]. With increase in water fraction the faint emission gradually got increased with a gradual red shift as discussed before. It may be due to the lowering of the band gap with increase in solvent polarity which is the expected characteristics of AIEE behavior. At water fraction above 80% the decrease in intensity is probably due to insolubility of the compound.

3.2.3. Time course of Fluorescence response to AIEE properties: Lifetime studies

To further confirm the AIE nature time resolved fluorescence spectra was taken where representative decay profiles of intensity (log scale) versus time (ns) are presented in the

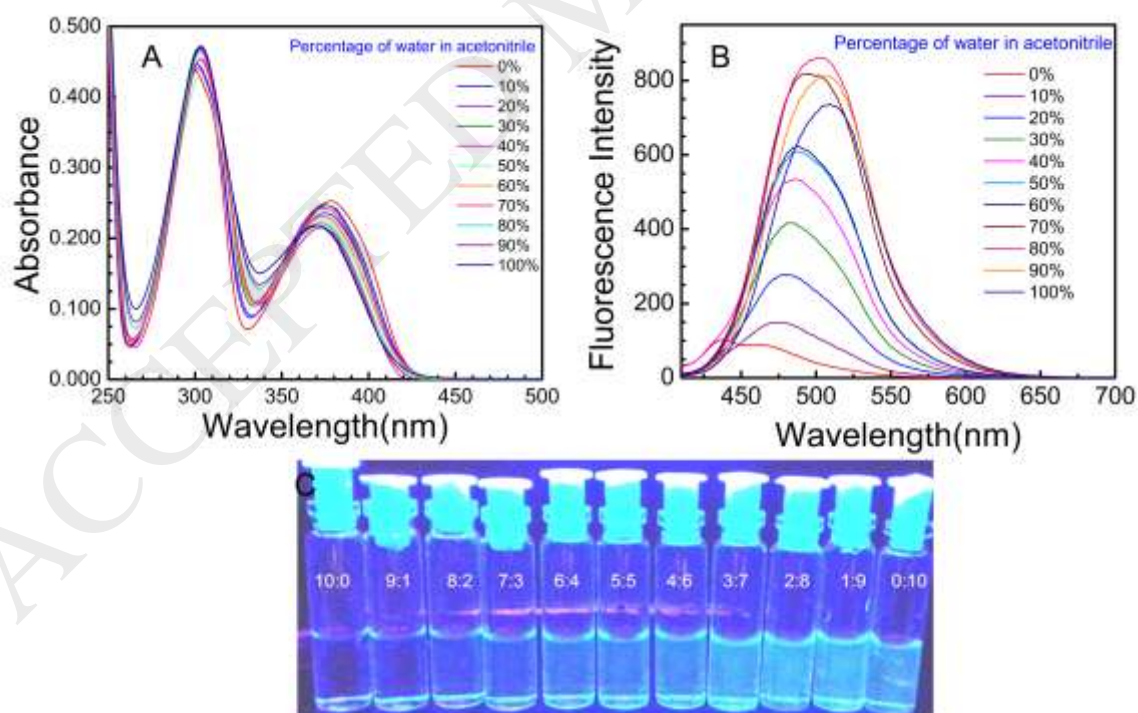


Fig. 1. AIEE spectral properties depicted by various fractions of hydrosols of compound **1**. A: Changes in absorption spectra, B: Changes in emission spectra, C: Naked eye AIEE characteristics under UV light (366 nm) (increasing water fractions from left to right)

Fig.2. and the corresponding data are summarized in Table 1. Compound **1** in free form was found to exhibit bi-exponential decay profile with average lifetime 0.86 ns in pure acetonitrile. The bi-exponential decay was also found to be the characteristic of fluorophore **1** in hydrosol form. The probable explanation of bi-exponential decay profiles of fluorophore **1** both the conditions indicate two different forms [30] i.e., the keto and enol form of the fluorophore 2-hydroxy quinoline-3-carbaldehyde in the excited state. The average life time (τ) of the hydrosol were found to be 1.91 ns and 1.54 ns for 50% and 80% water fraction. The life times of the hydrosols are much more than pure acetonitrile solution of compound **1** which is 0.86 ns. 80% water containing hydrosol flourished more than its 50% counterpart but stability of 50% water containing hydrosol in excited state is the maximum as depicted from the fluorescence life time studies. Pure water solution of the fluorophore **1** exhibited a life time value of 1.46 ns which is less than 80% hydrosol which indicates at reduction in stability of the hydrosol in the excited state with increasing water fraction. From the average lifetime of the hydrosols and their quantum yield the radiative rate constant (K_r) and the non radiative rate constants (K_{nr}) were calculated from the following equations:

$$\tau^{-1} = K_r + K_{nr} \quad \text{--- (6)}$$

$$K_r = \frac{\phi}{\tau} \quad \text{--- (7)}$$

The data related to decay profile have been depicted in the table where α_1 and α_2 represent the

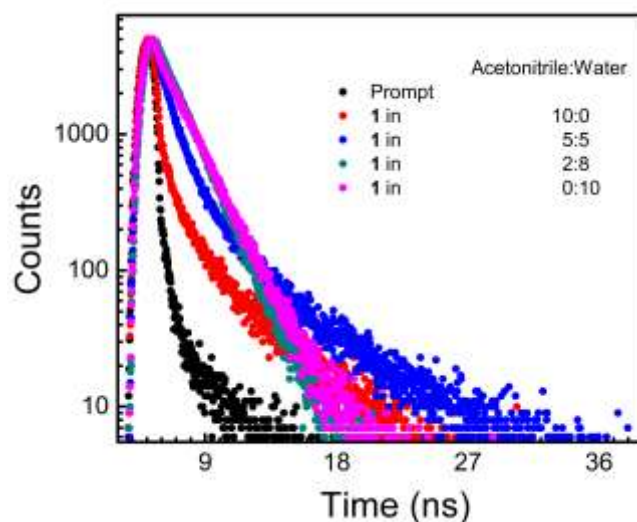


Fig. 2. Decay profile of fluorophore **1** in acetonitrile and other hydrosol fractions.

relative amplitude of the decay components in the excited state and other terms have their usual meaning as mentioned in the text. From the life time study it is evident that at 0 % water fraction the non radiative decay constant was much higher compared to radiative decay constant but with increase in water fraction the non radiative decay constant decreased from 1.155 ns to 0.615 ns. This fact supports that through the RIM mechanism is operative in aggregate solution the non-radiative decay process is getting hampered enhancing the fluorescence emission.

3.2. Effect of viscosity and solvent polarity on emission spectra

Effect of viscosity on emission spectra was observed by increasing viscosity of the solvent by increasing fraction of glycerol in ethanol. With increasing viscosity in solvent, the emission intensity also got enhanced up to 75% and drops down at pure glycerol medium (Fig. 3). Enhancement due to increase in viscosity is probably due to restricted intramolecular motion (RIM) in a more viscous solvent and reducing the nonradiative emissive pathways. In pure glycerol the intensity drops due to agglomeration of particles in the medium of maximum viscosity.

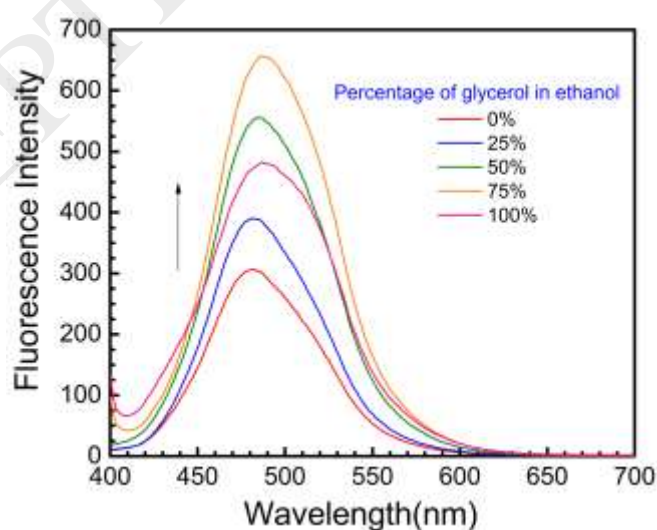


Fig. 3. Emission spectra of compound **1** in various fractions of glycerol in ethanol.

While studying effect of solvent on the absorption and emission spectra of the quinoline moiety **1** the spectra were recorded in various solvent with solute concentration of 5×10^{-5} M (Fig. 4). In absorption studies there is no remarkable change on the two absorption bands. The higher energy band II remained more or less unchanged whereas slight changes were visible on the lower energy band I, but no clear-cut trend of solvent dependency of the compound **1** on the solvent polarity was observed. But noticeable changes can be found in the emission spectrum with different solvents. The wavelength at emission maximum for chloroform, toluene, dimethyl formamide, dimethyl sulfoxide centered between 461.5 nm to 463 nm. Emission maxima for hexane and acetonitrile were at 426.5 and 436 nm respectively.

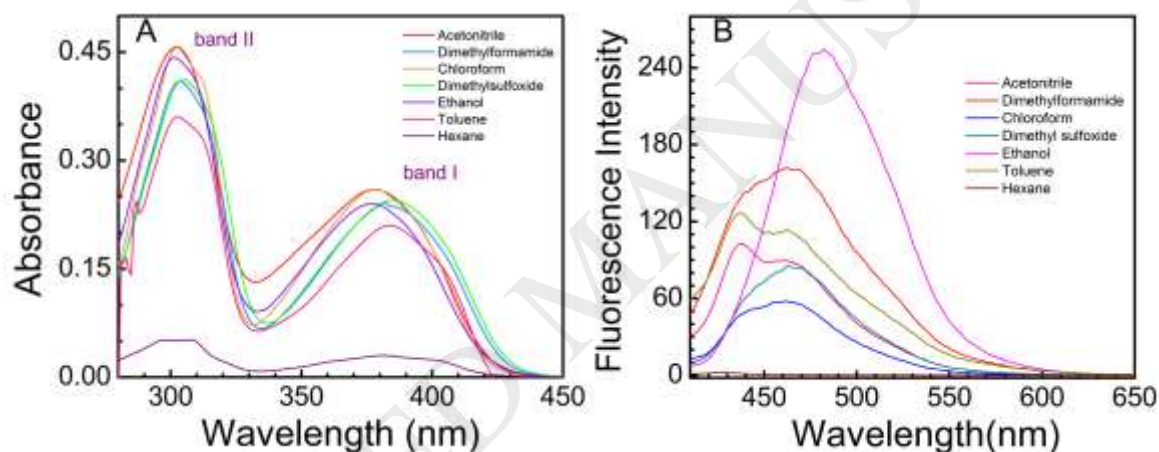


Fig. 4. Solvent effect on absorption and emission spectrum of compound **1** (5×10^{-5} M).

Only for polar protic ethanol emission maximum was observed at a longer wavelength of 482.5 nm. The fluorophores are generally weak fluorescent in hydrophilic (polar) solvents and high fluorescent in hydrophobic (non-polar) solvents but in some cases the reverse trend (strong fluorescence in protic solvents and weak fluorescence in aprotic solvents) is observed like acridine and 7-methoxy-4-methylcoumarin [41, 42]. In case of our compound **1** the reverse trend was noticed where maximum emission intensity was observed in polar protic ethanol followed by aprotic dimethyl formamide, acetonitrile, toluene dimethyl sulfoxide, chloroform and hexane. The solvatochromism data are depicted in Table 2.

3.3. Anion recognition

3.3.1. Naked eye sensing

ACCEPTED MANUSCRIPT

Naked eye experiment of anion interaction was carried out in acetonitrile. To a solution of compound **1** (9×10^{-4} M) in acetonitrile 15×10^{-4} M anions (F^- , Cl^- , Br^- , I^- , AcO^- , $H_2PO_4^-$, HPO_4^- , NO_3^- , AsO_2^- , N_3^-) were added. It was observed that for F^- ion the colorless receptor solution changed to yellow color indicating a host-guest type of interaction between charge neutral receptor **1** and charged F^- ion. No such obvious change of color was observed with other anions (Cl^- , Br^- , I^- , AcO^- , $H_2PO_4^-$, HPO_4^{2-} , NO_3^- , AsO_2^- , N_3^-) which may be due to feeble

ACCEPTED MANUSCRIPT

Table 2. Parameters related to UV-vis and emission spectra of compound **1** in various solvents.

Solvent	Dielectric constant (ϵ) at 20 °C	λ_{\max} at Band I (nm)	λ_{\max} at Band II in nm.	λ_{\max} at emission maxima	Intensity at emission maxima
Acetonitrile	20.7	378	302	436	102.79
Dimethylformamide	36.7	382	303	462.5	161.64
Chloroform	4.81	378	302	461.5	57.92
Dimethylsulfoxide	46.7	385	305	463	85.04
Ethanol	24.5	377	301	482.5	254.12
Toluene	2.38	384	303	462.5	113.39
Hexane	1.89	382	307	426.5	1.97

or no interaction with the receptor (Fig. 5). This colorimetric sensing indicated some sort of host-guest interaction between the neutral receptor and charged anion F^- . Similar experiment was also performed under ultraviolet radiations of 366 nm where weak turn on emission was visible with F^- in comparison to free receptor **1**. No turn on effect was evident in case of interaction of compound **1** with other anions viz. Cl^- , Br^- , I^- , AcO^- , $H_2PO_4^-$, HPO_4^{2-} , NO_3^- , AsO_2^- , N_3^- .



Fig. 5. Colorimetric changes of compound **1** (9×10^{-4} M) in acetonitrile in presence of 15×10^{-4} M anions A: naked eye B: under UV light at 366 nm.

3.3.2. ^1H NMR studies

^1H NMR spectra of the receptors **1** was recorded in DMSO- d_6 both in the presence and absence of fluoride ion to know the nature of interaction between them. ^1H NMR spectrum of the receptor **1** showed -OH proton signal at δ 12.2 ppm (Fig. 6). To investigate anion binding properties of the receptor **1**, the ^1H NMR spectral change caused by the addition of F^- as tetrabutylammonium salts were studied. The addition of F^- was increased gradually from 0 to 1 equivalent. On adding 1 equivalent of F^- the proton signals corresponding to -OH proton at δ 12.2 disappeared.

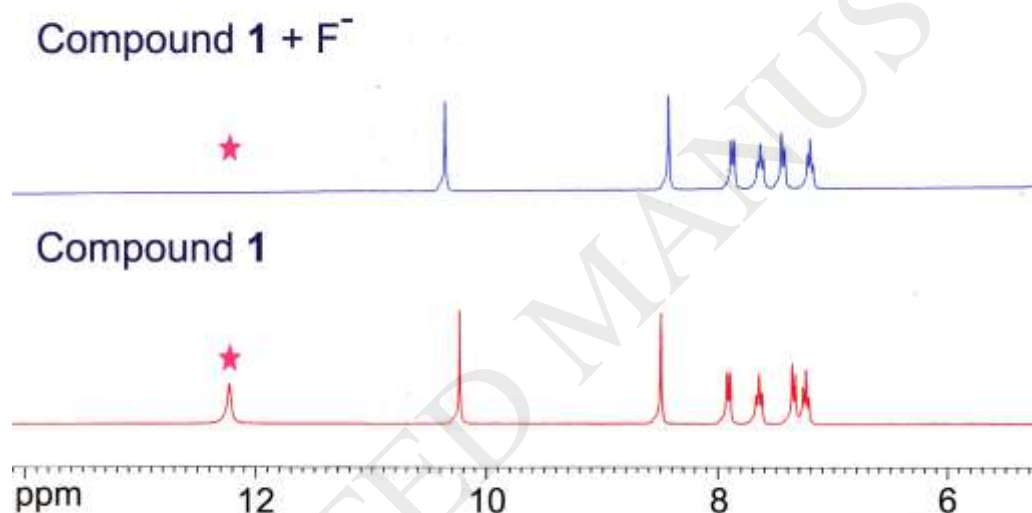


Fig. 6. Partial ^1H -NMR studies before and after addition of 1 equivalent of F^- to receptor **1**.

The disappearance of the proton signal is possibly due to H-bonding interactions between slightly acidic -OH protons and F^- ions. As a result of this interaction the electron density in the ring increases thus shielding also increases which further caused an upward shift of field for the ring protons.

3.3.3 Absorbance studies on anionic interaction

To corroborate with colorimetric and ^1H -NMR studies anionic interaction was investigated through absorption studies. The receptor itself showed two absorption maxima at 378 nm and 302 nm in acetonitrile medium.

UV-vis studies were done with 10×10^{-3} M standard solution of anions in acetonitrile. To 5×10^{-5} M solution of receptor **1** in acetonitrile in the cuvette 10 equivalent of each of the anions were added and changes in the absorption spectra were noticed (Fig. 7).

The free receptor exhibited absorption band at 378 and 302 nm which corresponds to two isomeric forms of the quinoline moiety. Upon excess addition of anions, the absorption band at 378 nm got drastically diminished and absorption band at 302 nm increased in intensity with a blue shift to 292 nm for F^- ion. There was insignificant change in the absorption band of the sensor negligible for other anions (Fig. 7) suggesting that the interaction is occurring only for F^- ion.

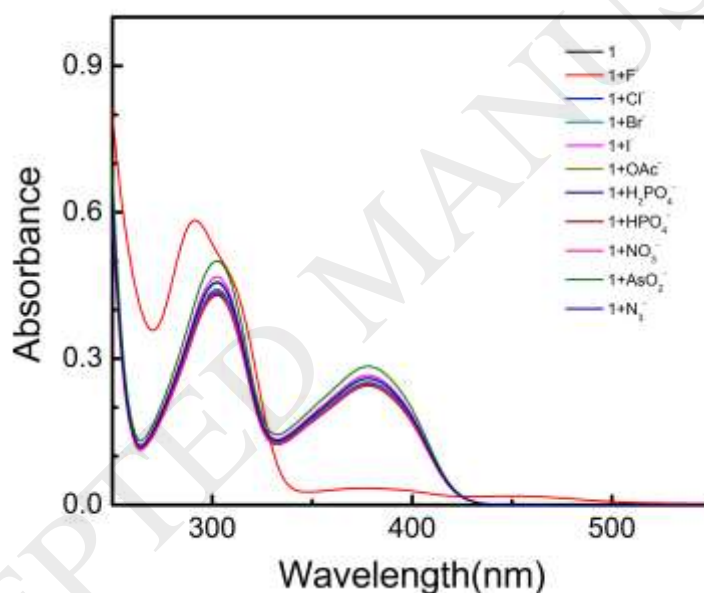


Fig. 7. Changes in absorption spectra of **1** (5×10^{-5} M) after addition of 10 equivalent of each anion.

UV-vis titration was performed with F^- ion in which 5×10^{-5} M solution of **1** in acetonitrile was titrated by gradual addition of F^- in acetonitrile upto 52×10^{-6} M (Fig. 8). The absorption band at 378 nm got gradually diminished and enhancement of the absorption band at 302 nm happened. Ultimately the absorption maximum at 302 nm outlives. Towards saturation a positive blue shift of the band at 302 nm to 292 nm occurred accordingly the faint colored solution of the receptor **1** changed to deep yellow color. The course of titration was associated with two

isosbestic points at 425 nm and 329 nm indicating equilibrium between receptor **1** and **1.F** complex formed in due course of titration. The obtained fact indicates at strong hydrogen bonding interaction and further deprotonation upon excess addition of F^- ion. All of these observation points at acidic nature of OH present in the receptor and highly basic nature of F^- ion.

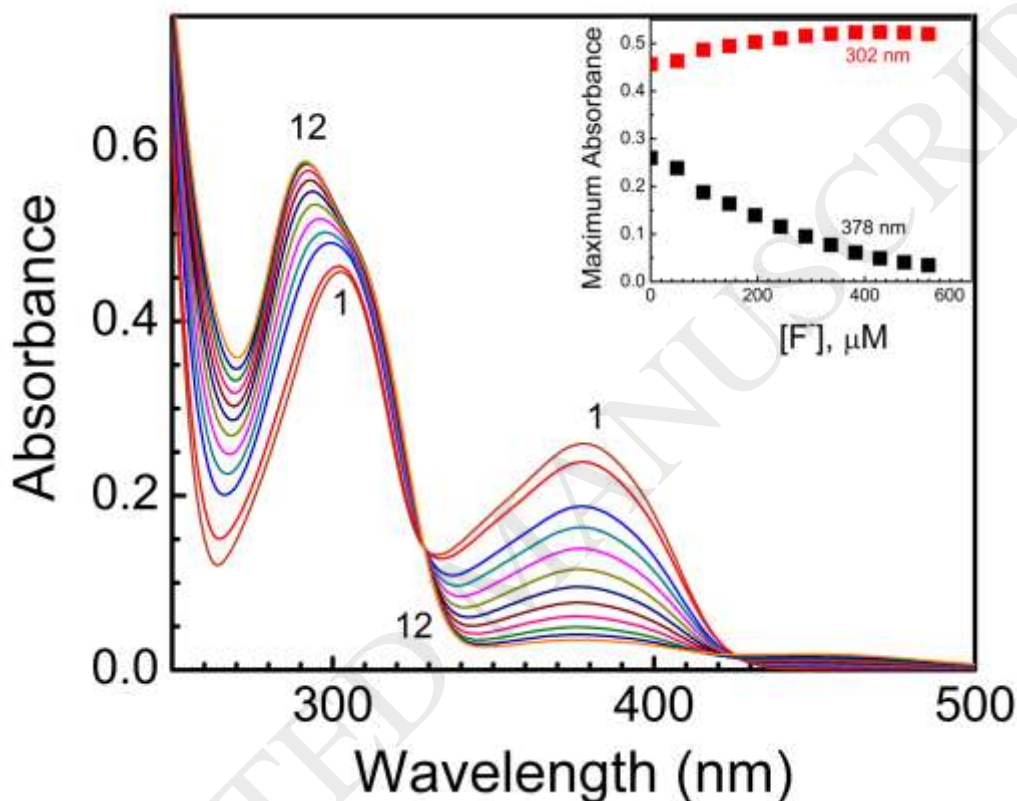


Fig. 8. Spectral titration of **1** (5.0×10^{-5} M) in CH_3CN (2 mL) (curve 1) with the addition of incremental amount of F^- (52×10^{-5} M) (curve 12). Inset: Variation of maximum absorbance with fluoride ion concentration in μM at 302 nm and 378 nm.

The extent of interaction was understood from the determination of binding constant from Benesi-hildebrand plot (Fig. 9) keeping in mind 1:1 complexation of **1** and F^- (which was indicative from 1H NMR studies and Jobs plot which is discussed a little later). The value of binding constant obtained is $2.641 \times 10^3 M^{-1}$. The value of binding constant indicates at the acidity of OH protons which are participating in anionic interaction.

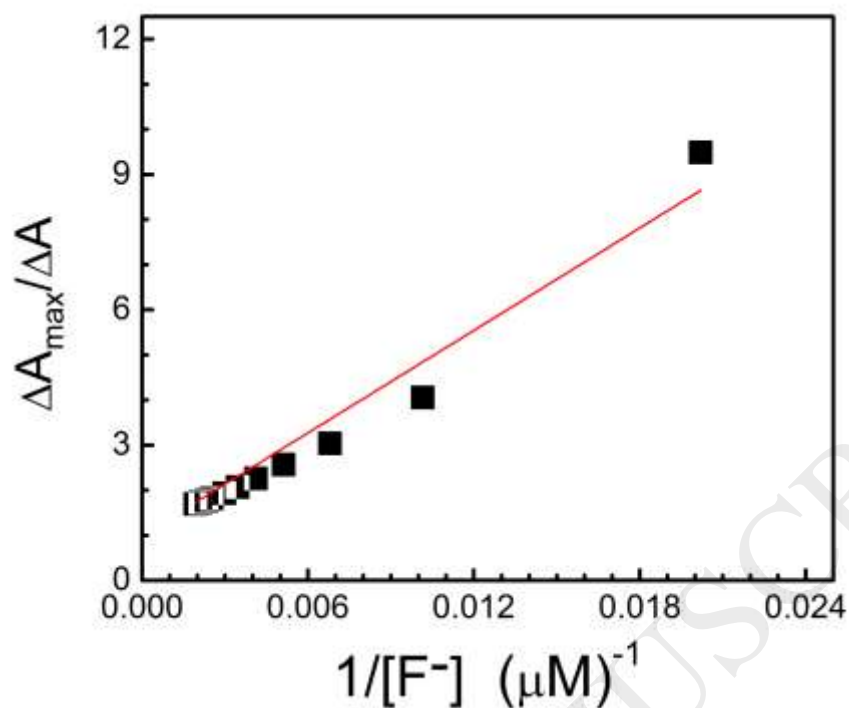


Fig. 9. Benesi-Hildebrand plot for binding of F^- ion with **1** (absorbance taken at 378 nm).

The detection limit of the receptor **1** towards F^- was determined from the calibration curve (Fig.10) as mentioned in the experimental section. The limit of detection (L.O.D) was determined to be as low as 4.09×10^{-6} M.

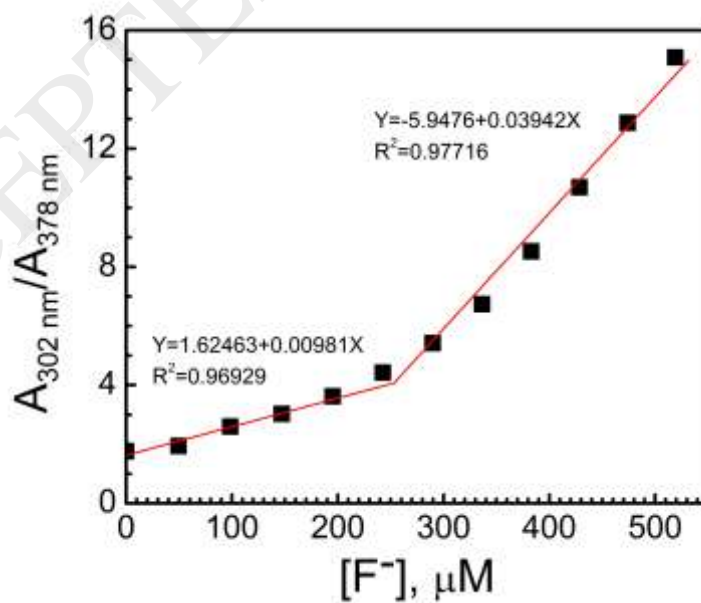


Fig. 10. Linear fit of ratiometric absorbance with increasing F^- concentration.

Job's method of continuous variation was employed to determine the stoichiometry of complex formation between anion F^- and compounds **1** using absorption profile. In our study, the inflection point was found to be at $\chi_{F^-}=0.49$. From this inflection point stoichiometry of the $F^-:1$ complex as calculated are $\sim 1:1$ (Fig. 11).

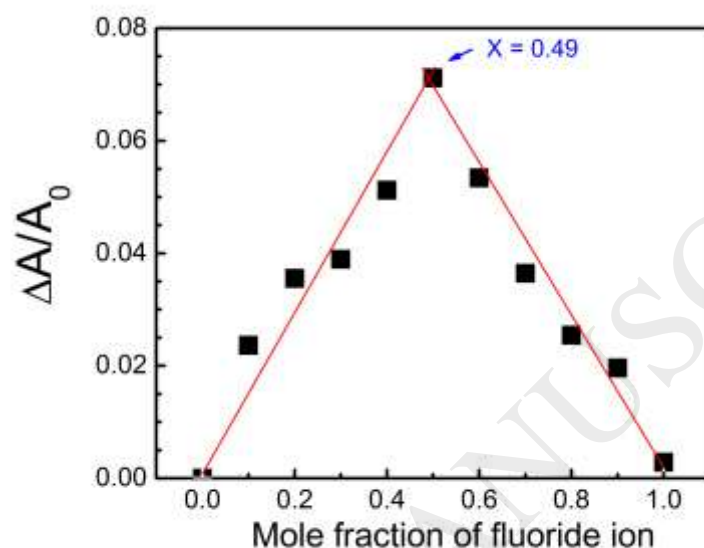


Fig. 11. Job's plot for binding of F^- ion with **1** (absorbance taken at 378 nm).

3.3.4. Emission Studies on anionic interaction

The receptor **1** showed two emission maxima at 436 nm and 461 nm when excited at 378 nm in acetonitrile medium (Fig. 12). The emission slit was kept at 5 nm and excitation slit was kept at 10 nm. The two emission bands correspond to two isomers of the quinoline moiety. On one-time addition of the 1×10^{-5} anions viz. F^- , Cl^- , Br^- , I^- , AcO^- , $H_2PO_4^-$, HPO_4^{2-} , NO_3^- , AsO_2^- , N_3^- to 1×10^{-5} of the solution of sensor **1** was done to monitor the selectivity of the sensor already noticed from absorption studies. The emission band of the free receptor at 436 nm and 461 nm showed fluorescence enhancement upon addition of F^- , whereas similar addition of other anions resulted in some minor changes in intensity of the existing emission spectra of the receptor.

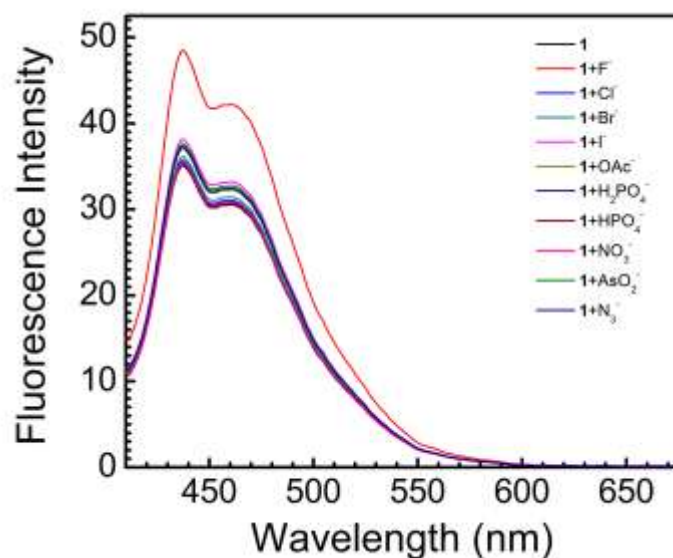


Fig. 12. Emission studies of 1×10^{-5} M solution receptor **1** with 1×10^{-5} M of anions.

The sensor **1** showed a time dependent enhancement of fluorescence intensity upon addition of F^- ions. To $10 \mu\text{M}$ solution of the receptor in acetonitrile $10 \mu\text{M}$ of F^- ions was added for kinetic study (Fig. 13). In the kinetic study the valley was obtained after 50 scans at an interval of 1 minute. At initial level the emission maxima both at 437.5 nm and 461 nm

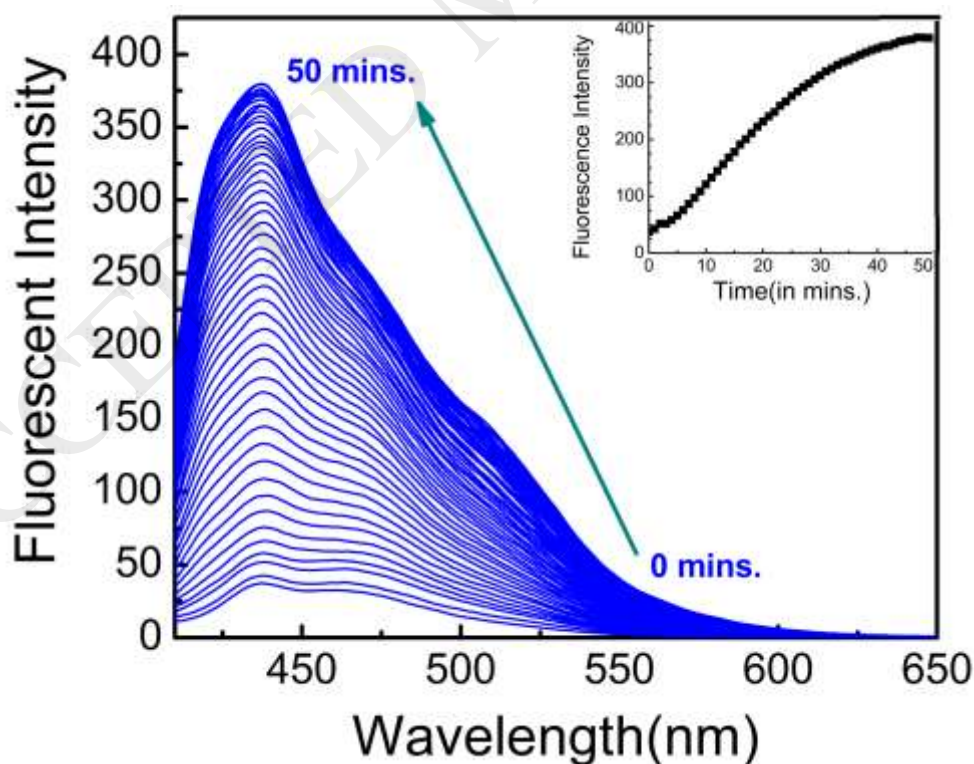


Fig. 13. Steady state increase in emission intensity of 1×10^{-5} M solution receptor **1** with 1×10^{-5} M of F^- with increase in time.

showed enhancement of emission intensity. As the time progress the band at 461 nm saturates while the band at 437.5 nm continued to show enhancement until stabilization. At the beginning two emission bands showed enhancement due to hydrogen bond formation of F^- with both the isomeric forms of ligand **1**. With progress of time a stable hydrogen bonded form outlives till the stability in enhancement with time was reached.

After attainment of stability in spectra with time fluorescence titration with incremental addition of F^- ion was performed. The emission band at 437.5 nm started to diminish in intensity with a positive Stoke shift to 496 nm where the intensity enhances until saturation upto addition of 155×10^{-5} M of F^- (Fig. 14). This phenomenon probably corresponds to deprotonation with increase in F^- ion concentration.

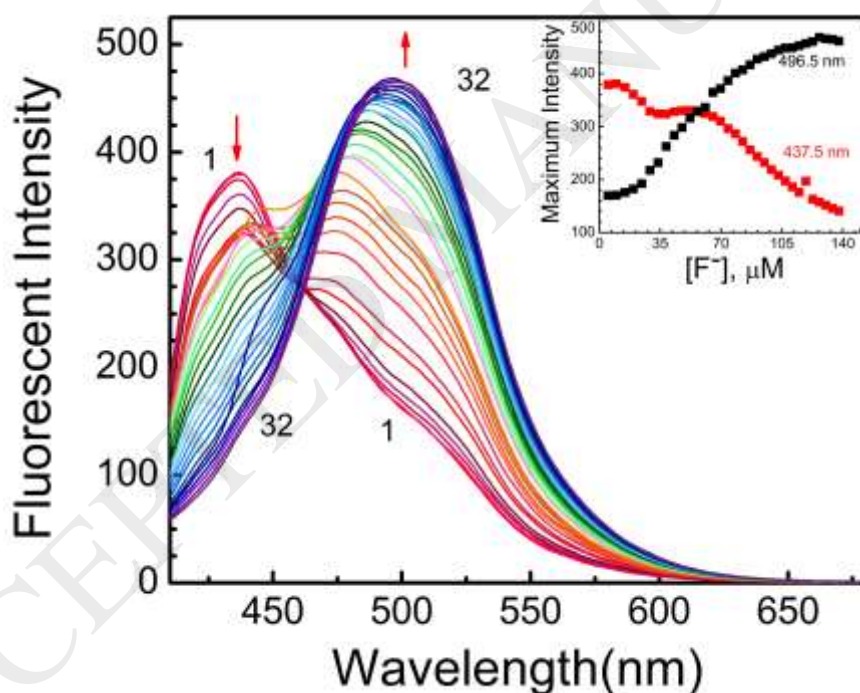


Fig. 14. Fluorescence titration of ligand **1** (1×10^{-5} M) after attainment of stability with time with F^- from 5×10^{-5} M (curve 1) to 155×10^{-5} M (curve 32) fluoride ion concentration. Inset: Variation of maximum intensity with fluoride ion concentration in μ M at 437.5 nm and 496.5 nm.

3.3.5. Fluorescence Lifetime studies on anionic interaction

In our life time studies representative decay profiles of intensity (log scale) versus time (ns) are presented in the Fig. 15 and the lifetime data are presented in Table 3. α_1 and α_2 represent

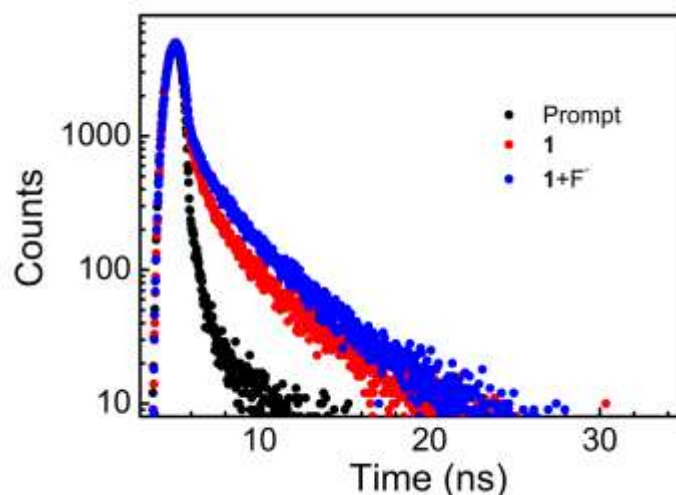


Fig. 15. Decay profile of fluorophore **1** in acetonitrile before and after interaction with F^- .

the relative amplitude of the decay components in the excited state. Lifetime signifies the average amount of time fluorophore herein compound **1** resides in the excited state during excitation. Moreover for multi-exponential decay, lifetime is a statistical average. As stated earlier compound **1** in free form was found to exhibit bi-exponential decay profile with a lifetime of 0.86 ns. In our experimental condition the fluorophore **1** upon binding with F^- also exhibited a bi-exponential decay and the lifetime value was increased, which provide two lifetime values like free fluorophore. Most probable explanation of this observation is that along with the presence of two different forms of the ligand [24] in the free form and presence of bound fluorophore along with trace amount of free fluorophore after anionic interaction. Lifetime value was increased from 0.86 ns to 1.03 ns. Increase in lifetime value indicated the stronger binding of fluorophore **1** with F^- in the experimental condition.

Table 3. Life time decay parameters of fluorophore **1** upon interaction with F^- ion.

Compounds	τ_1 (ns)	(α_1)	τ_2 (ns)	(α_2)	Average life time (τ) of the fluorophore 1 (ns)	χ^2
1	0.17	78.47	3.38	21.53	0.86	1.34
1 + $[F^-]$	0.15	68.8	2.98	31.20	1.03	1.46

3.3.6. Selectivity of fluoride sensing: Competitive experiment

Competitive experiments were carried out after attainment of stability with time. To the mixture of receptor **1** (1×10^{-5} M) and F^- (5×10^{-5} M) various anions (5×10^{-5} M) were added to find their effect on the F^- interaction with ligand **1**. In the competitive there were no or slight changes in the fluorescent intensity at 437.5 nm (Fig. 16). Thus selectivity and uniqueness of sensor **1** for fluoride ion sensing was once again established.

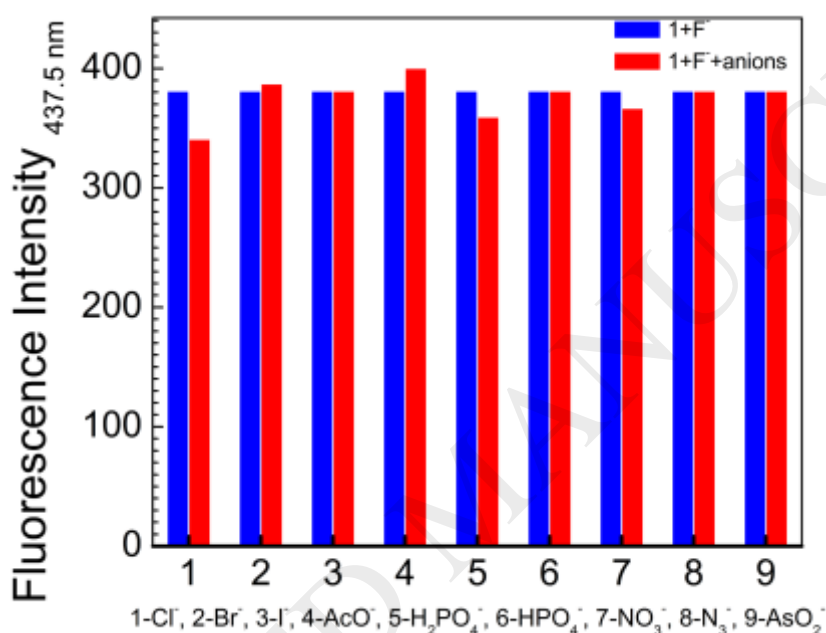


Fig. 16. Competitive experiment with various anions (5×10^{-5} M) to the mixture of receptor **1** (1×10^{-5} M) and F^- (5×10^{-5} M).

3.4. Interaction of compound **1** with BSA

The compound **1** was found to interact with protein bovine serum albumin (BSA) in tris-HCl (pH=7.4) medium. The quinoline **1** (5.0×10^{-5} M) exhibited two absorption maxima at 302 nm and 369 nm (Fig. 17). Absorption intensities at the maxima got reduced upon addition of BSA solution (Upto 3.81×10^{-7} M). Two clear isosbestic points were noted at 320 nm and 347 nm indicating an equilibrium between free and BSA bound compound **1**.

In fluorescence titration experiment 3.81×10^{-7} M BSA was titrated with increasing concentration of compound **1** upto 10×10^{-5} M (Fig. 18.). BSA exhibited emission maxima at

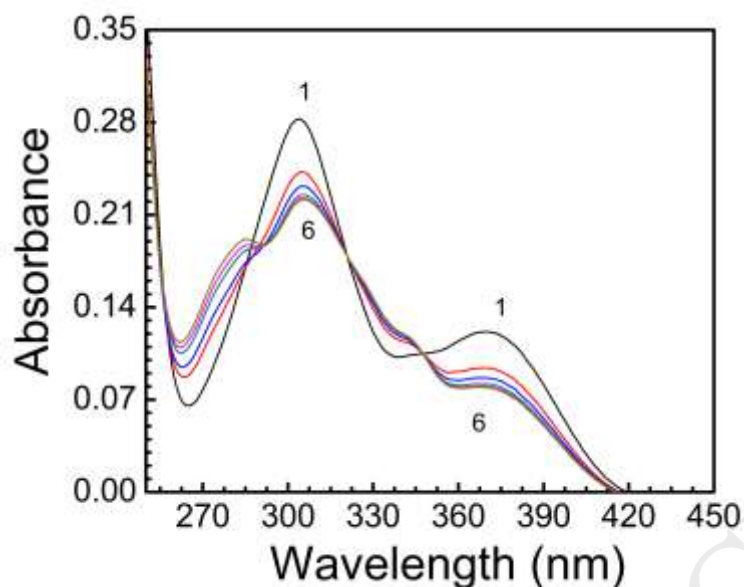


Fig. 17. UV-vis titration spectra of **1** (5.0×10^{-5} M) (curve 1) with 3.81×10^{-7} M BSA (curve 6).

346.5 nm in tris-HCl (pH=7.4) medium which upon interaction with compound **1** got quenched. The association constant was evaluated from the fluorescence titration of BSA with compound **1** (mentioned later). From the fluorescence titration we have also estimated the Stern Volmer quenching constant using the Stern-Volmer equation since there was reduction of BSA fluorescence on interaction with the said compound.

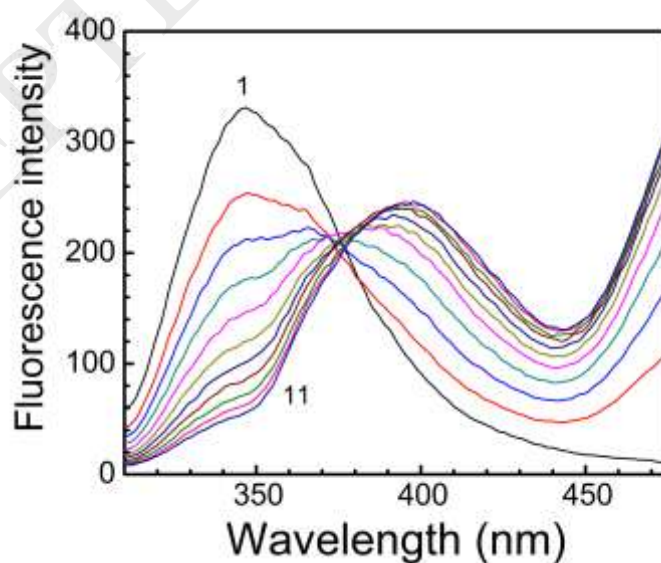


Fig. 18. Emission titration spectra of BSA with **1**. (Curve 1) 3.81×10^{-7} M BSA. (Curve 11) 10×10^{-5} M of compound **1**.

The Stern-Volmer equation is:

$$\frac{I_0}{I} = 1 + K_{sv}[X] \quad \text{--- (8)}$$

where, I_0 and I are the fluorescence intensities of the free fluorophore and complex between fluorophore and quencher, $[X]$ is the concentration of the quencher ion and K_{SV} is the Stern–Volmer quenching constant. K_{SV} is indicative of the accessibility of the bulky quencher to the fluorophore **1**. The slope of the I_0/I versus $[X]$ plot yields the value of K_{SV} . The plot of I_0/I versus $[X]$ obtained for the quenching is more or less a linear one throughout indicating the quenching to be static in nature. From the slope obtained in the plot the K_{SV} value obtained is $4.01 \times 10^5 \text{ M}^{-1}$ for quenching of emission intensity of free BSA upon binding with compound **1** (Fig.19). The quenching efficiencies were calculated to be 82.22%. Binding constant of protein-**1** complex formation was obtained from emission profile with the help of Benesi-Hildebrand plot (Fig. S3) where $\Delta I_{max}/\Delta I$ was plotted as a function of $1/[C]$ as mentioned in the experimental section. The binding constants came out to be $4.21 \times 10^5 \text{ M}^{-1}$ from the slope which indicates at strong interaction between compound **1** and protein BSA.

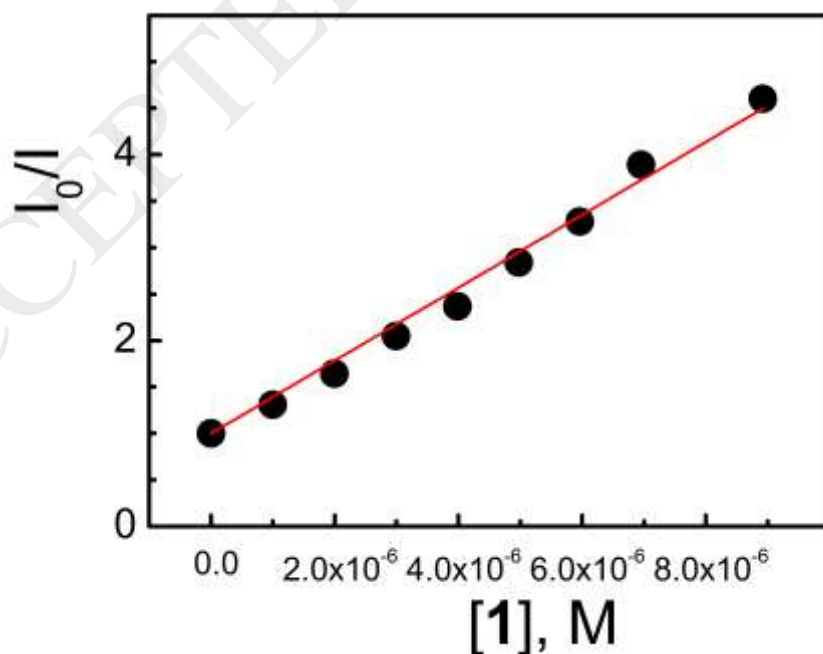


Fig. 19. Stern-Volmer plot for quenching of fluorescence intensity of BSA at 346.5 nm.

The fluorescence life time experiment was also performed in tris-HCl buffer to further investigate the nature of interaction. Decay curve of free BSA and bound BSA with compound **1** were obtained (Fig. S4). Both the free and the bound curves are of bi-exponential in nature with life time of 5.35 ns and 3.22 ns respectively. The results indicate at reduction of life time of the protein BSA upon interaction with compound **1**. We can conclude that a ground state one between BSA and compound **1**. The detail of the life time experiments have been depicted in Table S1.

4. Conclusion

In our study we have established a simple 2-hydroxyquinoline-3-carbaldehyde moiety as an effectual anionic chemosensor for F^- also showing aggregation induced enhancement in emission intensity as a hydrosol in acetonitrile-water mixture. The receptor studied was found to be selective sensor for F^- as colorimetric sensing, spectrophotometric, spectrofluorimetric, lifetime and competitive experiments through our studies. The interaction with F^- resulted in time dependant enhancement of fluorescent intensity of the receptor **1**. The quinoline based sensor **1** was found to interact with protein BSA in tris-HCl medium showed quenching of intensity of BSA protein. Our study has focused on various photophysical properties of quinoline based carbaldehyde which would help the researchers in further studies with this important precursor for many organic compounds in the future work.

5. Acknowledgements

AC gratefully acknowledges financial supports from Science and Engineering Research Board, DST, Government of India (SERB No.SR/FT/CS-116/2010) and SD gratefully acknowledges the financial assistance provided by the University Grant Commission (UGC), New Delhi, India [F. No. 43-243/2014 (SR), MRP-MAJORCHEM-2013-37991]. NC thanks UGC, Government of India for Senior Research Fellowship. SB acknowledges UGC, Government of India for RGNF Senior Research Fellowship. DM is thankful to DST-SERB

(PDF/2016/002123), India for financial assistance. We also thank the Department of Chemistry, Maulana Azad College, Kolkata, West Bengal, India and Department of Chemistry, Jadavpur University, Kolkata, India.

References

- [1] Z. Zhao, J. W. Y. Lam, B. Z. Tang, Tetraphenylethene: a versatile AIE building block for the construction of efficient luminescent materials for organic light-emitting diodes, *J. Mater. Chem.* 22 (2012) 23726–23740.
- [2] J. Zhou, Z. Chang, Y. Jiang, B. He, M. Du, P. Lu, Y. Hong, H. S. Kwok, A. Qin, H. Qiu, Z. Zhao, B. Z. Tang, From tetraphenylethene to tetranaphthylethene: structural evolution in AIE luminogen continues, *Chem. Commun.* 49 (2013) 2491–2493.
- [3] D. Ding, K. Li, B. Liu, B. Z. Tang, Bioprobes based on AIE fluorogens, *Acc. Chem. Res.* 46 (2013) 2441–2453.
- [4] J. Luo, Z. Xie, J. W. Y. Lam, L. Cheng, H. Chen, C. Qiu, H. S. Kwok, X. Zhan, Y. Liu, D. Zhu, B. Z. Tang, Aggregation-induced emission of 1-methyl-1,2,3,4,5-pentaphenylsilole, *Chem. Commun.* 0 (2001) 1740–1741
- [5] Z. Zhao, B. He, B. Z. Tang, Aggregation-induced emission of siloles, *Chem. Sci.* 6 (2015) 5347–5365.
- [6] W. Z. Yuan, Y. Gong, S. Chen, X. Y. Shen, J. W. Y. Lam, P. Lu, Y. Lu, Z. Wang, R. Hu, N. Xie, Efficient solid emitters with aggregation-induced emission and intramolecular charge transfer characteristics: molecular design, synthesis, photophysical behaviors, and OLED application, *Chem. Mater.* 24 (2012) 1518–1528.

- [7] A. Malakar, M. Kumar, A. Reddy, H. T. Biswal, B. B. Mandal, G. Krishnamoorthy, Aggregation induced enhanced emission of 2-(2'-hydroxyphenyl)benzimidazole, *Photochem. Photobiol. Sci.*, 15 (2016) 937-948
- [8] Z. Zhu, J. Qian, X. Zhao, W. Qin, R. Hu, H. Zhang, D. Li, Z. Xu, B. Z. Tang, S. He, Stable and Size-Tunable Aggregation-Induced Emission Nanoparticles Encapsulated with Nanographene Oxide and Applications in Three-Photon Fluorescence Bioimaging, *ACS Nano* 10 (1) (2016) 588–597.
- [9] B. Xu, J. Zhang, H. Fang, S. Ma, Q. Chen, H. Sun, C. Im, W. Tian, Aggregation induced enhanced emission of conjugated dendrimers with a large intrinsic two-photon absorption cross-section, *Polym. Chem.* 5 (2014) 479-488.
- [10] Y. Duan, C. Ju, G. Yang, E. Fron, E. Coutino-Gonzalez, S. Semin, C. Fan, R. S. Balok, J. Cremers, P. Tinnemans, Y. Feng, Y. Li, J. Hofkens, A. E. Rowan, T. Rasing, J. Xu, Aggregation Induced Enhancement of Linear and Nonlinear Optical Emission from a Hexaphenylene Derivative, *Adv. Funct. Mat.*, 26 (48) (2016) 8968–8977.
- [11] S. Pramanik, V. Bhalla, M. Kumar, Hexaphenylbenzene-based fluorescent aggregates for ratiometric detection of cyanide ions at nanomolar level: set-reset memorized sequential logic device, *ACS Appl. Mater. Interfaces* 6 (2014) 5930–5939.
- [12] S. S. Mati, S. Chall, S. C. Bhattacharya, Aggregation-induced fabrication of fluorescent organic nano rings: selective biosensing of cysteine and application to molecular logic gate, *Langmuir* 31 (2015) 5025–5032.
- [13] H.S. Horowitz, The 2001 CDC recommendations for using fluoride to prevent and control dental caries in the United States, *J. Public Health Dent.* 63 (1) (2003) 3-8.
- [14] S. Dey, B. Giri Fluoride fact on human health problems: a review, *Med. Clin. Rev.* 2(1) (2016) 1-6.

- [15] X. Zheng, W. Zhu, D. Liu, H. Ai, Y. Huang, Z. Lu, Highly selective Colorimetric/Fluorometric Dual-Channel Fluoride ion Probe and Its Capability of Differentiating Cancer Cells, *ACS Appl. Mater. Interfaces* 6 (2014) 7996-8000
- [16] K. Kangaraj, K. Pitchumani, Highly selective "Turn-On" Fluorescent and Colorimetric Sensing of Fluoride Ion Using 2-(2-Hydroxyphenyl)-2,3-dihydroquinolin-1H)-one based on Excited-State Proton Transfer, *Chem. Asian J.* 9 (2014) 146-152.
- [17] G. Feng, L. Geng, T. Wang, J. Li, X. Yu, Y. Wang, Y. Li, D. Xie, Fluorogenic and chromogenic detection of biologically important fluoride anion with Schiff-bases containing 4-amino-1,8-naphthalimide unit, *J. Lumin.* 167 (2015) 65-70.
- [18] P. Zhang, C. Li, H. Zhang, Y. Li, X. Yu, L. Geng, Y. Wang, X. Zhen, Z. Ma, Fluorogenic and chromogenic detection of biologically important fluoride anion in aqueous media with fluorescein-linked hydrogen-bonding receptor via "off-on" approach, *J. Incl. Phenom. Macrocycl. Chem.* 81 (2015) 295-300.
- [19] S. Velmathi, V. Reena, S. Suganya, S. Anandan, Pyrrole based Schiff bases as colorimetric and fluorescent chemosensors for fluoride and hydroxide anions, *J. Fluoresc.* 22 (2012) 155-162.
- [20] E. Saika, P. Dutta, B. Chetia, A Novel Benzimidazolyl-based Receptor for the recognition of Fluoride and Cyanide ion, *J. Chem. Sci.* 129 (2017) 1-7.
- [21] A. Agostini, M. Milani, R. Martinez-Manez, Azo Dyes Functionalized with Alkoxysilyl Ethers as Chemodosimeters for the Chromogenic Detection of the Fluoride Anion, *Chem. Asian J.* 7 (2012) 2040-2044.
- [22] M. Chandel, S. M. Roy, D. Sharma, S. K. Sahoo, A. Patel, P. Kumari, R. S. Dhale, K. S. K. Ashok, J. P. Nandre, U. D. Patil, Anion recognition ability of a novel azo dye derived from 4-hydroxycoumarin, *J. Lumin.* 154 (2014) 515-519.

- [23] R. H. Valleyjos, O. A. Roveri, Alkaloid iInhibition of Yeast Respiration-Prevention by Ca^{2+} , *Biochem. Pharmacol.* 21 (1972) 3179-3182.
- [24] U. Knogh-Hanser, V. T. Chuang, M. Otagiri, Practical Aspects of the Ligand binding and Enzymatic Properties of Human Serum Albumin, *Biol. Pharm. Bull.* 25 (2002) 695-704.
- [25] D. C. Carter, X. M. He, S. H. Munsor, P. D. Twigg, K. M. Gernemt, M. B. Broom, T. Y. Miller, Three dimensional Structure of Human Serum Albumin, *Science* 244 (1989) 1195-1198.
- [26] D. C. Carter, J. X. Ho, Structure of Serum Albumin, *Adv. Protein Chem.* 45 (1994) 153-203.
- [27] T. Peters Jr., All about Albumins: Biochemistry, Genetics and Medical Applications, Academic Press: San Diego, 1996.
- [28] J. F. Foster, Albumin Structure, Fuction and Uses, Pregamon Press, Oxford, 1977.
- [29] B. F. Abdel-Wahab, R. E. Khidre, Abdelbasset A. Farahat, A-A. S. El-Ahl, 2-Chloroquinoline-3-carbaldehydes: synthesis, reactions and applications, *Arkivoc I* (2012) 211-276.
- [30] M. C. Mandewale, B. Thorat, Y. Nivid, R. Jadhav, A. Nagarsekar, R. Yamgar, Synthesis, structural studies and antituberculosis evaluation of new hydrazone derivatives of quinoline and their Zn(II) complexes, *J. Saudi Chem. Soc.* (2016), <http://dx.doi.org/10.1016/j.jscs.2016.04.003>.
- [31] Z. C. Liu, Z. Y. Yang, T. R. Li, B. D. Wang, Y. Li, M. F. Wang, DNA-binding, antioxidant activity and solid-state fluorescence studies of copper(II), zinc(II) and nickel(II) complexes with a Schiff base derived from 2-oxo-quinoline-3-carbaldehyde, *Transition Met. Chem.* 36 (2011) 489–498.

- [32] A. Srivastava, R. M. Singh Vilsmeier-Haack reagent: A facile synthesis of 2-chloro-3-formyl quinolines from N-arylamides and transformation into different functionalities. *Ind. J. Chem.* 44B (2005) 1868-1875.
- [33] W. H. Melhuish, Quantum efficiencies of fluorescence of organic substances: effect of solvent and concentration of the fluorescent solute¹, *J. Phys. Chem.* 65 (1961) 229-235.
- [34] D. F. Eaton, Reference material for fluorescent measurement *Pure Appl. Chem.*, 1988, 60, 1107-1114.
- [35] H. A. Benesi and J. H. Hildebrand, *J. Am. Chem. Soc.* 71(8) (1949) 2703-2707.
- [36] P. Job, Formation and Stability of Inorganic Complexes in Solution, *Ann. Chim. Appl.* 9 (1928) 113-203.
- [37] S. Das, S. Parveen, A.B. Pradhan, An insight into the interaction of phenanthridine dyes with polyriboadenylic acid: Spectroscopic and thermodynamic approach, *Spectrochim. Acta Part A: Mol. Biomol. Spectrosc.* 118 (2014) 356-366.
- [38] M. C. Mandewale, B. R. Thorat, R. S. Yamgar, Synthesis and anti-mycobacterium study of some fluorine containing Schiff bases of quinoline and their metal complexes, *Der Pharma Chemica.* 7 (2015) 207-215.
- [39] Y. Fang, X. Yi, W. Qin, Y. Zhang, Y. Liao, Synthesis and Antitumor Activities of Some 2-Oxo-quinoline-3-Schiff Base Derivatives, *Asian J. Chem.* 26 (2014), 7449-7451.
- [40] J. Mei, Y. N. Hong, J. W. Y. Lam, A. J. Qin, Y. H. Tang, B. Z. Tang, Aggregation-Induced Emission: The Whole Is More Brilliant than the Parts *Adv. Mater.* 2014, 26, 5429 – 5479

[41]A. Kellmann, Intersystem crossing and internal conversion quantum yields of acridine in polar and nonpolar solvents, *J. Phys. Chem.* 81 (1977) 1195–1198.

[42]S. Uchiyama, K. Takehira, T. Yoshihara, S. Tobita, T. Ohwada, Environment- sensitive fluorophore emitting in protic environments, *Org. Lett.* 8 (2006) 5869–5872.

ACCEPTED MANUSCRIPT